The Astrophysical Journal, 694:L136–L139, 2009 April 1 doi:10.1088/0004-637X/694/2/L136

PHYSICAL PROPERTIES OF FOUR SZE-SELECTED GALAXY CLUSTERS IN THE SOUTHERN COSMOLOGY SURVEY

Felipe Menanteau and John P. Hughes
Department of Physics & Astronomy, Rutgers University, 136 Frelinghuysen Road, Piscataway, NJ 08854, USA
Received 2008 November 21; accepted 2009 February 3; published 2009 March 13

ABSTRACT

We present the optical and X-ray properties of four clusters recently discovered by the South Pole Telescope (SPT) using the Sunyaev–Zel'dovich effect (SZE). The four clusters are located in one of the common survey areas of the southern sky that is also being targeted by the Atacama Cosmology Telescope (ACT) and imaged by the CTIO Blanco 4 m telescope. Based on publicly available $griz$ optical images and *XMM-Newton* and *ROSAT* X-ray observations, we analyze the physical properties of these clusters and obtain photometric redshifts, luminosities, richness, and mass estimates. Each cluster contains a central elliptical whose luminosity is consistent with SDSS cluster studies. Our mass estimates are well above the nominal detection limit of the SPT and ACT; the new SZE clusters are very likely massive systems with $M \gtrsim 5 \times 10^{14}\ M_{\odot}$.

Key words: cosmic microwave background – cosmology: observations – galaxies: clusters: general – galaxies: distances and redshifts – large-scale structure of universe

1. INTRODUCTION

Galaxy clusters serve as important cosmological probes as their formation and evolution rate depend on cosmological parameters and the kinematics of the dark matter. They are the observational counterparts of dark matter halos, and their abundances and masses as a function of redshift are quite sensitive to the growth of structure in the universe offering a potentially powerful probe of dark energy (Carlstrom et al. 2002). Galaxy clusters also harbor a significant fraction of the visible baryons in the universe. Hydrogen gas, heated as it falls into the dark-matter potential well of a cluster, forms an intracluster medium too hot to be bound by individual galaxies. The hot intracluster gas leaves an imprint on the cosmic microwave background radiation (CMBR) though the Sunyaev–Zel'dovich effect (SZE) (Sunyaev & Zel'dovich 1972) in which CMB photons are inverse-Compton scattered by the hot intracluster gas. It is this SZE signal that two new ground-based mm-band telescopes, the Atacama Cosmology Telescope (ACT) (Kosowsky 2006; Fowler et al. 2007) and the South Pole Telescope (SPT) (Ruhl et al. 2004), have been designed to detect through its frequency-dependence: these experiments will measure intensity shifts of the CMBR corresponding to a decrement below and an increment above the "null" frequency around 220 GHz. Both telescopes are now actively acquiring data over large areas of the southern sky that will ultimately cover several hundreds to thousands of square degrees.

Recent results from the SPT collaboration (Staniszewski et al. 2008) have yielded the first blind detection of SZE clusters in one of the common southern survey regions centered near right ascension $05^{\rm h}30^{\rm m}$ and declination -53°. This area has also been scanned by the ACT and has been optically imaged in the optical ($griz$) with the CTIO Blanco 4 m telescope as part of the Blanco Cosmology Survey (BCS) (Menanteau et al. 2008; Staniszewski et al. 2008). Prompted by these results, here we present a detailed study of the physical properties of these first four SZE-detected clusters based on publicly available optical imaging and archival X-ray data. Throughout this paper we assume a flat cosmology with $H_0 = 100h$ km s^{-1} Mpc^{-1}, $h = 0.7$, and matter density $\Omega_m = 0.3$.

2. SZE OPTICAL COUNTERPARTS

The positions of the four SZE-selected clusters reported by the SPT team are contained within the region surveyed by the BCS in 2005 and 2006. These observations have been publicly available for about a year or more now. We have processed and analyzed them using an independent software pipeline developed by us at Rutgers University. We refer the reader to Menanteau et al. (2008) where we provide a full description of the observing strategy, pipeline and data products, and some results on new massive galaxy clusters discovered in the BCS survey field centered near 23 hr. Here we use the identical software pipeline to generate data products from which we characterize the optical properties of the four SZE clusters. First, we identify the optical counterparts, which appear as clearly visible overdensities of early-type galaxies near the sky locations of the SZE decrements (see Table 1 from Staniszewski et al. 2008). Roughly centered within each overdensity is a bright elliptical, which we take to be the brightest cluster galaxy (BCG). In Figure 1 we show the gri color images of the four systems, centered on the location of the BCG. Each system shows a dominant population of early-type galaxies with very similar colors that can easily be identified by visual inspection. In all cases, the offset between the BCG and the SZE decrement, shown as red ellipses and green crosses respectively, is less than ~ 30 arcsec.

2.1. Photometric Redshift Determination

We determine photometric redshifts from the four-band optical images using BPZ (Benítez 2000) following the same procedure as in Menanteau et al. (2008). To avoid contamination by non-cluster members we use the BCG to estimate the photometric redshift of each system. The BCG is, by definition, indisputably part of the cluster, resides in a quasi-central location, and always provides the strongest signal and the best colors since such galaxies are generally several times brighter than L^* at any given redshift. Moreover, the luminosities and particularly the colors of BCGs are well constrained as they are very bright elliptical galaxies dominated by old metal-rich stellar populations for which multicolor spectral energy distribution (SED) fitting techniques are well suited yielding precise and

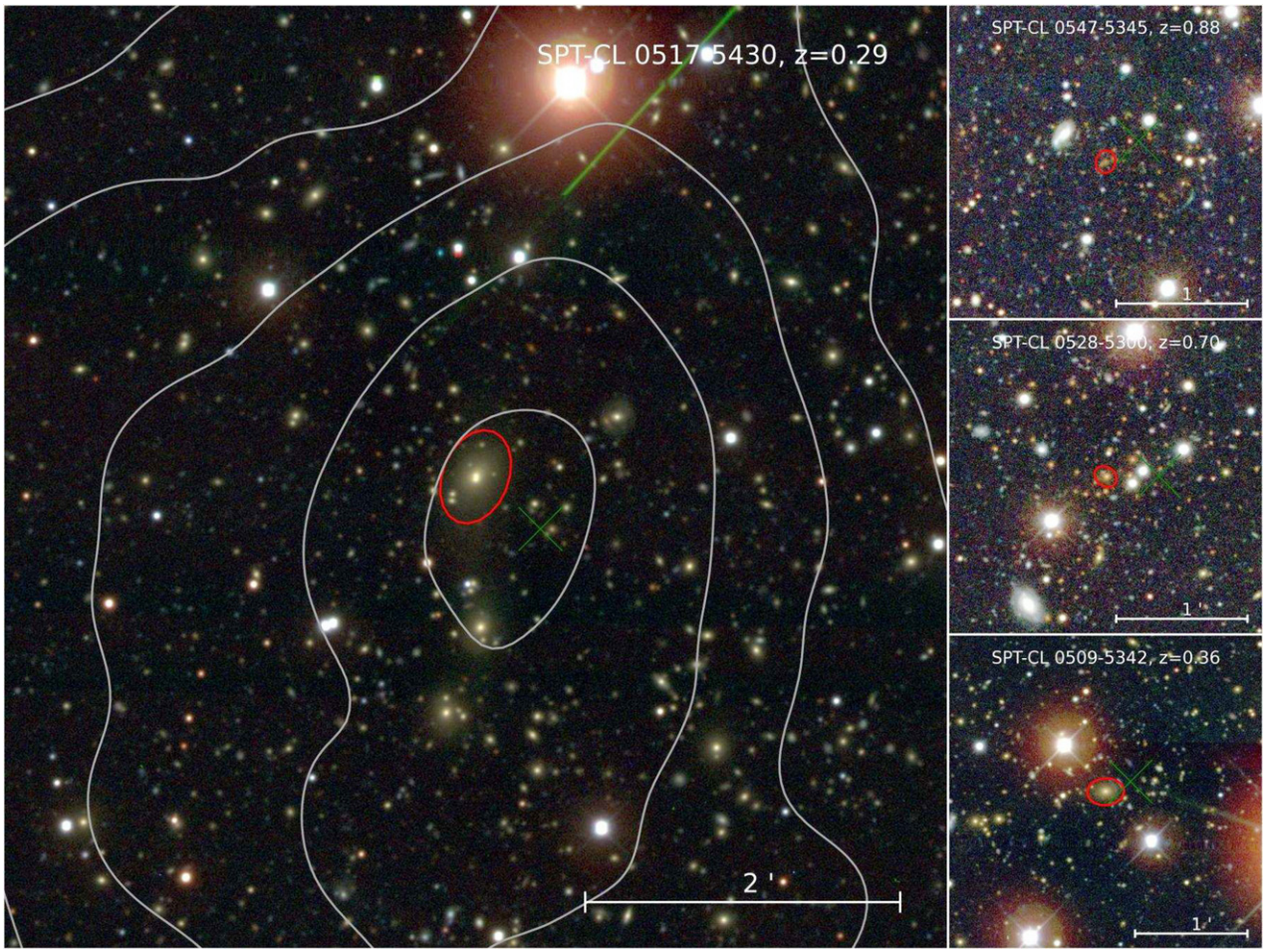

Figure 1. Composite *gri* color image of the four SPT SZE-selected clusters from the data. Green crosses show the position of the SZE decrement from Staniszewski et al. (2008) for each system. The red ellipses denote the position of the BCG and show as well the SExtractor Kron radius. For cluster SPT-CL 0517−5430 (Abell 0520, main panel) we show the *XMM-Newton* X-ray isointensity contour levels (starting near the center at a value of 1×10^{-4} counts s^{-1} $pixel^{-1}$ and decreasing going outward by factors of 2.5).

Table 1
Cluster Optical/X-ray Properties and Mass Estimates

ID	R.A.	Decl.	z_{photo}	N_{200}^{gal}	L_{200} ($10^{12} L_\odot$)	L_{BCG} (10^{10} $L_\odot$)	$M(L_{200})$ (10^{15} $M_\odot$)	L_X(0.1–2.4 keV) (10^{44}ergs^{-1})	$M(L_X)$ (10^{15} $M_\odot$)
SPT-CL 0517−5430	05:16:37.4	−54:30:01.5	$0.27^{+0.02}_{-0.02}$	168.9 ± 15.3	6.53 ± 0.15	31.20	1.7	3.5 ± 0.5	0.8
SPT-CL 0509−5342	05:09:21.4	−53:42:12.3	$0.36^{+0.02}_{-0.02}$	76.1 ± 9.2	2.24 ± 0.05	9.07	0.4	2.2 ± 0.8	0.6
SPT-CL 0528−5300	05:28:05.3	−52:59:52.8	$0.70^{+0.03}_{-0.02}$	69.3 ± 9.8	8.62 ± 1.20	23.00	$\geqslant 2.1$	< 5.5	< 1.1
SPT-CL 0547−5345	05:46:37.7	−53:45:31.1	$0.88^{+0.08}_{-0.04}$	12.7 ± 3.7	1.99 ± 0.25	17.90	$\geqslant 0.4$	4.7 ± 2.3	1.0

Note. Physical properties of SZE selected clusters in the SCS regions. Redshifts represent the photometric redshift from the bright elliptical in the center of the cluster with $\pm 1\sigma$ limits. The cluster position is based on the BCG.

reliable results. In the bottom panel of Figure 2 we show the output BPZ photometric redshift probability density function (pdf) for each BCG. The differences between the BPZ Bayesian and maximum likelihood (ML) predicted redshifts are small ($\delta z \simeq 0.01$) in all cases and therefore we will employ ML photometric redshifts hereafter as the addition of a prior is not justified when, as is the case here, the BCG SEDs are fitted unambiguously. We note that occasionally BCGs host radio-loud active galactic nuclei (Best et al. 2007). Although we have no indication of this, if any of our BCGs do harbor AGNs then we would expect some blueing of the colors causing our photo-z's to be slightly overestimated.

Only one of the clusters, SPT-CL 0517−5430, has been previously reported; it is the optically rich cluster Abell S0520 (Abell et al. 1989) which is also the X-ray cluster RXC J0516.6−5430 (Böhringer et al. 2004). Its published spectroscopic redshift of $z = 0.294$ (Guzzo et al. 1999) is in excellent agreement with our photometric redshift for that BCG, $z = 0.27 \pm 0.02$, but somewhat different from the value of $z = 0.35$ quoted by Staniszewski et al. (2008) for the cluster which came from the peak of their photo-z distribution of red-sequence galaxies using the same BCS imaging. In Table 1 we present the clusters' optical positions based on the BCG locations and photometric redshifts with 1σ uncertainties.

2.2. BCG Luminosities

The range in brightness of BCGs has been observationally established from galaxy clusters in the SDSS up to redshifts

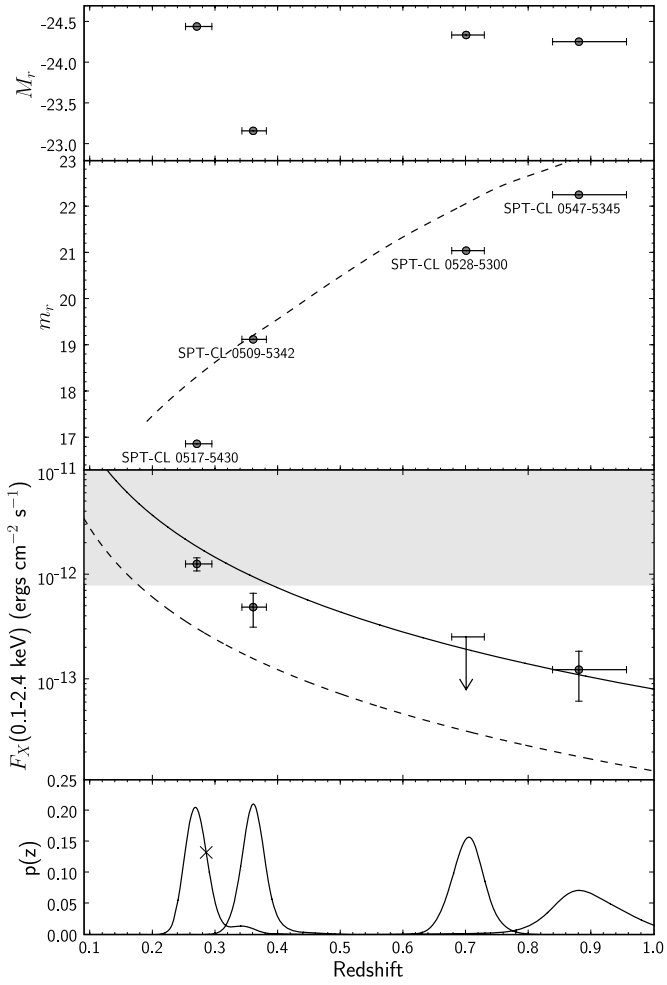

Figure 2. Absolute (upper panel) and observed (second panel) *r*-band magnitude of each BCG as a function of its photometric redshift. The dashed line represents the modeled observed *r*-band magnitude of BCGs according to Loh & Strauss (2006). In the third panel we show the clusters' soft X-ray flux as a function of redshift. The solid and dashed curves represent the expected X-ray fluxes for clusters with mass of $M_{200} = 1 \times 10^{15}\ M_{\odot}$ and $3 \times 10^{14}\ M_{\odot}$ respectively. The bottom panel shows the photo-z probability distribution function for each BCG and with a cross at the location in the curve for SPT-CL 0517–5430's spectroscopic redshift. Error bars in the figure represent $\pm 1\sigma$ deviations drawn from the probability functions.

of 0.36 (see, e.g., Loh & Strauss 2006; Koester et al. 2007). This can be used to determine whether the BCGs we identify in the SZE clusters have luminosities consistent with SDSS BCGs. In Figure 2 (the second panel from top) we show the total *r*-band observed magnitude of each cluster's BCG as a function of redshift compared to a parameterization of the observed *r*-band magnitudes of SDSS BCGs (dashed line) (Figure 7 in Loh & Strauss 2006). The curve corresponds to the simple prescription $M^* - 1.5$ where M^* is taken from Blanton et al. (2003) and the model includes passive evolution with redshift. We have extrapolated the SDSS BCG luminosity model beyond $z = 0.36$ as there is overwhelming evidence that ellipticals in clusters have passively evolved since $z \simeq 1$ (Blakeslee et al. 2003; Lidman et al. 2008; Mei et al. 2009). We see from the figure that in all cases the BCGs in the SZE clusters are below the model curve (i.e., are intrinsically brighter) and we take this as strong evidence in support of them being bona fide BCGs. It is worth noting that SPT-CL 0509−5342 at $z = 0.36$ is the least luminous of the four, just slightly brighter than the luminosity predicted by the model. As we will see in the next section, this cluster also has a lower mass and X-ray luminosity compared to the other systems. In Figure 2 we also show the range of absolute magnitudes of the BCGs as a function of redshift. Here we again see that SPT-CL 0509−5342 is the least luminous object, $\simeq 1$ mag fainter than the other BCGs which all have about the same luminosity.

3. CLUSTER MASS ESTIMATIONS

The new SZE experiments aim to deliver mass-selected samples of galaxy clusters out to large redshifts which can be used to probe the growth of structure in the universe and to study cluster physics. Current *N*-body plus hydrodynamics simulations (Motl et al. 2005; Nagai 2006; Sehgal et al. 2007) predict robust scaling relations between the SZE signal (i.e., the *y*-distortion due to inverse Compton scattering) and cluster mass. However, a fundamental step before using SZE clusters as cosmological probes is to observationally establish the relationship between y and mass using mass estimates independent of the SZE measurements. SZE-selected clusters will almost surely be the focus of intense efforts to obtain mass estimates using X-ray images and spectra, weak and strong lensing, and velocity dispersions. In the following, we present the first independent mass estimates for these new SZE-selected clusters from archival optical and X-ray data.

3.1. Optical Cluster Masses

Here we use optically observed parameters of galaxies to predict the cluster mass from weak lensing richness–mass scaling relations established from the SDSS (Johnston et al. 2007; Reyes et al. 2008). We apply the state-of-the-art mass tracer (Reyes et al. 2008) built from the SDSS maxBCG cluster sample (Koester et al. 2007) of $\simeq$ 13,000 optically selected clusters. Here we briefly describe our procedure and refer the reader to our earlier study (Menanteau et al. 2008) for complete details. The quantities, $N_{200}^{\rm gal}$, L_{200}, and $L_{\rm BCG}$, are the observational values needed as input to the cluster mass scaling relation. The cluster richness, $N_{200}^{\rm gal}$, is the number of E/S0 galaxies within R_{200} with colors and luminosities that satisfy specific conditions for membership. R_{200} is the estimated cluster size defined as the radius where the cluster galaxy density is $200\Omega_m^{-1}$ times the mean space density of galaxies in the present universe. Similarly, L_{200} is the total rest-frame integrated *r*-band luminosity of all member galaxies included in $N_{200}^{\rm gal}$ and $L_{\rm BCG}$ is the rest-frame *r*-band luminosity of the BCG. Reyes et al. (2008) provide power-law functions for both the luminosity–mass and richness–mass relations (see Section 5.2.1 in their paper), although here we only use the relation based on luminosity, which should be more robust than that based on richness. In Table 1 we present the cluster mass estimates and luminosities where $M(L_{200})$ is the mass observational equivalent of $M_{200\bar{\rho}}$[1]. For the two higher redshift clusters, SPT-CL 0528−5300 at $z = 0.70$ and SPT-CL 0547−5345 at $z = 0.88$, we quote lower-limit estimates as some fraction of low-luminosity galaxies fall below our magnitude limit ($i \simeq 22.5$). If we make the assumption that the two higher redshift clusters have luminosity functions that are similar to SPT-CL 0517−5430 at $z = 0.29$, then we estimate that we are missing 15% and 58% of the luminosity for SPT-CL 0528−5300 and SPT-CL 0547−5345,

[1] $M_{200\bar{\rho}}$ is the halo mass enclosed within a radius of spherical volume within which the mean density is 200 times the critical density.

respectively. The mass estimates in Table 1 include these corrections.

3.2. X-ray Properties and Masses

The nearby cluster SPT-CL 0517−5430 has accurate measurements of its X-ray luminosity ($L_{\rm bol} = 9.2 \pm 1.2 \times 10^{44}$ erg s^{-1}) and temperature ($kT = 7.5 \pm 0.3$ keV) from *XMM-Newton* observations (Zhang et al. 2006). There is also a hydrostatic mass estimate of $M_{500} = 6.4 \pm 2.1 \times 10^{14}\ M_{\odot}$ (note this is at an overdensity of 500 times the critical density). The cluster's X-ray morphology is strongly elongated: it has an axial ratio of 1.4–1.7 with its major axis aligned ∼14° from north (see Figure 1).

We utilize the *ROSAT* All Sky Survey (RASS) to obtain X-ray information on the other three clusters. As noted by Staniszewski et al. (2008), faint RASS sources lie close to the locations of SPT-CL 0509−5342 and SPT-CL 0547−5300. For purposes of determining X-ray fluxes and luminosities we will assume that these RASS sources are indeed the X-ray counterparts to the SZ clusters. Starting with the raw X-ray photon event lists and exposure maps from the MPE *ROSAT* Archive[2] we determined count rates for the band covering PI channels 52 to 201. Extraction regions were optimized to obtain all detected source photons (a radius of 3′ was sufficient) and, for the background estimation, to reduce statistical fluctuations (using an annular region between 5′ and 25′). The X-ray source position was used for the two SZ clusters with apparent counterparts; for SPT-CL 0528−5300, the quoted SZ position was used to derive upper limits.

The background-subtracted count rates (SPT-CL 0509−5342: 0.025 counts s^{-1}; SPT-CL 0528−5300: $<$ 0.015 counts s^{-1}; SPT-CL 0547−5345: 0.007 counts s^{-1}) were converted to fluxes assuming a hard thermal spectrum ($kT \sim 5$ keV) and accounting for each cluster's Galactic absorbing column density (Dickey & Lockman 1990); values fell in the range 6.1×10^{20} atoms cm^{-2} to 7.8×10^{20} atoms cm^{-2} for all sources. A k-correction was also applied to convert fluxes to the standard 0.1–2.4 keV *ROSAT* band in the rest frame of each cluster. These fluxes are plotted in Figure 2 (the second panel from bottom). The upper limit for SPT-CL 0528−5300 is at 2σ and the soft 0.1–2.4 keV band flux for SPT-CL 0517−5430 was converted from the bolometric luminosity quoted by Zhang et al. (2006). We denote the region (at the high-flux end) that corresponds approximately to the Bright Source Catalog from the RASS. Also shown are curves of the expected X-ray fluxes for clusters with masses of $M_{200} = 1 \times 10^{15}\ M_{\odot}$ (solid) and $3 \times 10^{14}\ M_{\odot}$ (dotted). These curves assume the low-redshift luminosity–mass (specifically L_X(0.1–2.4 keV) vs. M_{200}) relation from Reiprich & Böhringer (2002) and, for simplicity, no redshift evolution. This scaling relation is also used to derive an X-ray mass estimate from the soft X-ray luminosity. Numerical values for these quantities are presented in the last two columns of Table 1.

4. SUMMARY

We have established that the central ellipticals associated with the four SZE clusters have luminosities consistent with those of BCGs from the SDSS. We have also determined cluster masses using two different mass estimators based on the luminosity of the optical galaxies and the X-ray-emitting gas. These mass tracers are reasonably consistent within the uncertainties given by the scatter in the X-ray luminosity–mass relation (∼0.2 in the log) and the estimated factor of 2 uncertainty in the mass derived from the optical luminosity of the galaxies (Menanteau et al. 2008). Based on this evidence, all four clusters are fairly massive ($M \gtrsim 5 \times 10^{14}\ M_{\odot}$) and therefore well above the nominal detection limit of both SPT and ACT (e.g., Sehgal et al. 2007). Although this is an important step in identifying the optical and X-ray counterparts to the SZ clusters, it cannot be considered definitive. In addition the RASS count rates could well be contaminated by X-ray emission from an AGN or other unrelated source. Thus the conservative reader could conclude that the X-ray luminosities and derived masses for the three higher redshift SPT sources represent upper limits to their true values. Approved *Chandra* observations will within the next year resolve any doubts about the X-ray emission of these clusters. Deeper optical imaging and spectroscopy should also be pursued in order to better constrain the masses of these clusters.

We thank the BCS team for the planning and execution of the CTIO Blanco observations that were used in this paper. We have made use of the *ROSAT* Data Archive of the Max-Planck-Institut für extraterrestrische Physik (MPE) at Garching, Germany, as well as results obtained from the High Energy Astrophysics Science Archive Research Center (HEASARC), provided by NASA's Goddard Space Flight Center. Financial support was provided by the National Science Foundation under the PIRE program (award number OISE-0530095). J.P.H. acknowledges financial support from NASA LTSA grant number NAG5-11414 and *XMM* grants NNX08AX72G and NNX08AX55G.

REFERENCES

Abell, G. O., Corwin, H. G., Jr., & Olowin, R. P. 1989, ApJS, 70, 1
Benítez, N. 2000, ApJ, 536, 571
Best, P. N., von der Linden, A., Kauffmann, G., Heckman, T. M., & Kaiser, C. R. 2007, MNRAS, 379, 894
Blakeslee, J. P., et al. 2003, ApJ, 596, L143
Blanton, M. R., et al. 2003, ApJ, 592, 819
Böhringer, H., et al. 2004, A&A, 425, 367
Carlstrom, J. E., Holder, G. P., & Reese, E. D. 2002, ARA&A, 40, 643
Dickey, J. M., & Lockman, F. J. 1990, ARA&A, 28, 215
Fowler, J. W., et al. 2007, Appl. Opt., 46, 3444
Guzzo, L., et al. 1999, Messenger, 95, 27
Johnston, D. E., et al. 2007, arXiv:0709.1159
Koester, B. P., et al. 2007, ApJ, 660, 221
Kosowsky, A. 2006, New Astron. Rev., 50, 969
Lidman, C., et al. 2008, A&A, 489, 981
Loh, Y.-S., & Strauss, M. A. 2006, MNRAS, 366, 373
Mei, S., et al. 2009, ApJ, 690, 42
Menanteau, F., Hughes, J. P., Jimenez, R., Hernandez-Monteagudo, C., Verde, L., Kosowsky, A., Moodley, K., & Roche, N. 2008, arXiv:0808.0214
Motl, P. M., Hallman, E. J., Burns, J. O., & Norman, M. L. 2005, ApJ, 623, L63
Nagai, D. 2006, ApJ, 650, 538
Reiprich, T. H., & Böhringer, H. 2002, ApJ, 567, 716
Reyes, R., Mandelbaum, R., Hirata, C., Bahcall, N., & Seljak, U. 2008, MNRAS, 390, 1157
Ruhl, J., et al. 2004, Proc. SPIE, 5498 (Bellingham, WA: SPIE), 11
Sehgal, N., Trac, H., Huffenberger, K., & Bode, P. 2007, ApJ, 664, 149
Sunyaev, R. A., & Zeldovich, Y. B. 1972, Comments Astrophys. Space Phys., 4, 173
Staniszewski, Z., et al. 2008, arXiv:0810.1578
Zhang, Y.-Y., Böhringer, H., Finoguenov, A., Ikebe, Y., Matsushita, K., Schuecker, P., Guzzo, L., & Collins, C. A. 2006, A&A, 456, 55

[2] ftp://ftp.xray.mpe.mpg.de/rosat/archive/.